

# Application of Computational Tear Flow Models to Smart Contact Lens Design

BEE 4530

Ryan Ashley, Marsela Fida, Jeffrey Li, Jeffrey Ly

## TABLE OF CONTENTS

1. Executive Summary .....	3
2. Introduction .....	4
3. Model Design .....	6
4. Results and Conclusions .....	10
5. Summary .....	16
6. References .....	17
7. Appendix .....	18

## **EXECUTIVE SUMMARY**

Millions of diabetics could benefit from a noninvasive and cheaper method for monitoring their blood glucose. A solution recently popularized by Google makes use of smart contact lenses featuring embedded glucose sensors which can detect and wirelessly transmit their measurements. This technology takes advantage of the glucose present in the aqueous humor of the human eye, which is proportional to the glucose present in the blood. The technology to produce such contact lenses is well established, but few numerical models are available to characterize the system. In particular the tear fluid dynamics responsible for distributing the glucose on the eye surface is not well understood. A model describing this behavior would facilitate the development, optimization, and prototyping of a smart contact lens that diabetic patients can depend on.

The goal of this project was to take advantage of 3D computational modeling to optimize glucose sensor placement on a contact lens. Several partial models were implemented to capture aspects of tear flow. An initial computational model was implemented based on a physical prototype [1]. It featured two inlets and one outlet, but did not provide a fully representative model with respect to physiological fluid flow on the eye. However, the experimental values from that project were sufficient to validate the physical accuracy of the computational model. Once this was established, a second model was implemented to take into account tear flow from the lacrimal gland across the eye to the lacrimal ducts. The locations of the inflow and outflow were selected to match physiological eye models [8]. A third model configuration simulates gravitational tear flow from the top eyelid to the bottom [7]. This was implemented as a constant inflow from the upper edge of the lens, and an outflow from the bottom edge. These three different models each captured a single aspect of physiological tear flow, so each predicted different profiles of fluid flow and glucose homogenization times. A combined model was created to weigh all these aspects of tear flow. This combined model was used to optimize locations for a glucose sensor based on glucose equilibration times at different locations within the model.

The models were demonstrated to be physically consistent and to be insensitive to the variable physiological parameters of tear flow velocity and glucose diffusivity, as well as to the computational parameter of mesh resolution. Subsequent experiments in the combined model yielded an optimized location for the glucose sensor that fit all the design criteria: avoiding occlusion of vision, providing adequate space for the sensor, and demonstrating fast equilibration time. A new sensor placement was proposed for subsequent design iterations of the lens. This location is closer to the upper eyelid than in the initial physical model. This optimized position decreased concentration equilibration time by 30%.

These results demonstrate the utility of computational models in the design of smart contact lenses. In particular the implementation of these models can allow very rapid prototyping of design concepts. These models demonstrate the viability of smart contact lenses and their potential as glucose monitoring solutions for diabetic patients, and to become a suitable alternative to lancet-based glucometers.

## INTRODUCTION

Diabetes is a chronic disease in which patients have improperly regulated blood sugar levels. In 2013, the American Diabetes Association reported that nearly 26 million children and adults suffer from diabetes in the United States. Diabetes is the primary cause of death for 71,382 Americans each year. Regardless of whether patients have Type 1 or Type 2 diabetes, it is important to continuously monitor their glucose level on a regular basis [6]. Current methods require pricking the finger for blood once every few hours. This can be a painful process, as the same skin must be pricked at each reading and the wounds opened in the pricking process are susceptible to infection. Additionally, current methods are inadequate because of their failure to give constant real-time readings of blood sugar. These tests can be costly; a package of 100 test strips can range anywhere from \$35 to \$156 dollars, which adds up to several thousand dollars per year for a single patient [6].

Several technologies have been explored in the search for a noninvasive glucose monitoring system. The list is extensive: near- and mid- infrared spectroscopies, optical coherence tomography, temperature-modulated localized reflectance, raman spectroscopy, polarization changes, ultrasound, fluorescence, thermal spectroscopy, and many others have all been candidates for commercialization for diabetic patients [2,3]. Although most of these technologies have the potential to be continuous monitoring systems, few are suitable for portable systems worn by outpatients. Many of these technologies also suffers from lack of specificity with respect to glucose monitoring. For example, for just near-infrared spectroscopy, physiological states of vasodilation, water content, carbon dioxide, atmospheric pressure, and more all can influence spectroscopic readings meant to describe glucose content [3].

Smart contact lenses are a promising noninvasive solution for glucose monitoring. They work by measuring glucose concentration with enzymatic sensors directly connected to miniaturized electronic circuits. The glucose concentrations in the tear fluid are correlated to glucose concentrations in the blood, so the measurements can be used to report the patient's approximate blood glucose in real time.

The best-known prototype smart contact lens was reported by Yao et al. in 2011 [1]. The model featured a glucose oxidase sensor embedded in a contact lens and mounted on a polydimethylsiloxane (PDMS) eye. Water containing varying glucose levels could be pumped into the system, and sensor readouts were obtained over time from attached electrodes, though the authors also discussed schemes for wirelessly transmitting the data. This early-stage model demonstrated that many of the functions and microcircuitry required for a smart contact lens were achievable. The study provided a wealth of valuable data on sensor responsiveness, lifespan, and sensitivity to tear composition. These data were crucial for preliminary assessment of the viability of the technology. However, the model itself could be better validated by more sophisticated fluid models capturing more aspects of tear dynamics.

Tear fluid dynamics have been modeled by several groups with several different methods. In one model, used in the Yao paper, the flow is generated by two diametrically placed inlets and an equidistant outlet, all spaced along the rim of the contact lens. These conditions allow controlled replacement of the fluid between the contact lens and the simulated eye surface. In a second model, the physiological configuration of the lacrimal apparatus determines the direction of flow on the eye surface [8]. The lacrimal apparatus consists of the excretory ducts, where tears are pushed onto the eye, and the lacrimal

canaliculi, where tears are drained from the eye. The excretory ducts are features on the lateral aspect (on the ear side) of the upper eyelids, while the lacrimal canaliculi are on the medial aspect (on the nose side) of the lower eyelids [8]. These inlet-outlet placements are an important consideration for a tear flow model. Finally, in a third model of tear flow, fluid released onto the eye rapidly flows along the edges of the upper eyelid as a meniscus resulting from surface tension [7]. This fluid is then uniformly spread onto the eye surface by the tear distributional system. Each of these models yields a slightly different flow pattern.

Computational models are a powerful design tool that provides a way to link tear flow models and sensing capabilities. Once the problem geometry is established and discretized into nodes and elements, the fluid dynamics can be implemented to simulate and predict changes in the system over time. A mass transport module can be implemented to generalize this to the glucose profile over time, equivalent to having sensors placed all over the domain. Post-simulation tools can allow interpretation of the data to include profiles over time at selected points on the lens. These tools allow rapid prototyping and testing of configurational changes to the contact lens components, which can accelerate the development of smart contact lens technology for facilitated blood sugar monitoring and management of diabetes in patients.

## MODEL DESIGN

### Problem Statement

Computational models of tear fluid dynamics and glucose dispersion across the eye, crucial to smart contact lens design, are not available in the literature.

### Design Objectives

- I. Computational modeling of tear fluid flow on the eye surface.
  - Computational modeling of glucose concentrations as a function of modeled tear flow.
- II. Validation of computational models.
  - Mesh convergence analysis to account for discretization error.
  - Sensitivity analysis to account for physiologically variable parameters.
  - Comparison of experimentally and computationally derived data.
- III. Optimization of sensor placement within the contact lens given the following design constraints:
  - Sensor cannot occlude vision - must be placed at least 3.75 mm from the center.
  - Sensor must fit on the contact lens - center must be placed at least 1 mm from the edge.
  - Fast glucose concentration equilibration time - less than 30 seconds.

### Schematic

A curved 3D geometry was designed using dimensions of the tear fluid reservoir from the physical model created by Yao et al. as shown in Figure 1 [1]. The top curved surface represents the contact lens boundary while the bottom surface represents the eye surface boundary. The shape between these surfaces is considered to be filled with tear fluid.

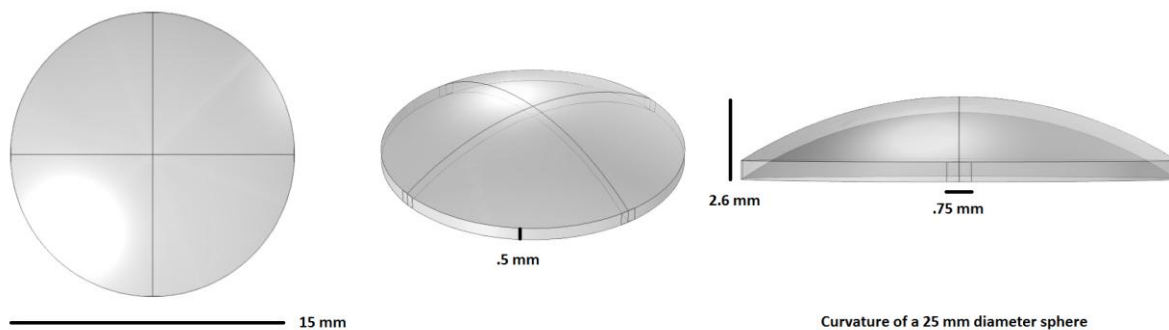


**Fig 1. Contact Lens Reservoir Geometry**

Next, three partial models were implemented based on three identified literature models of tear flow. The literature models are diagrammed in Figure 2. The models differ in several ways, but most notably in the effective inlet-outlet configurations of the moving fluid. The inlets and outlets positions were distilled from each model and incorporated into three computational models.

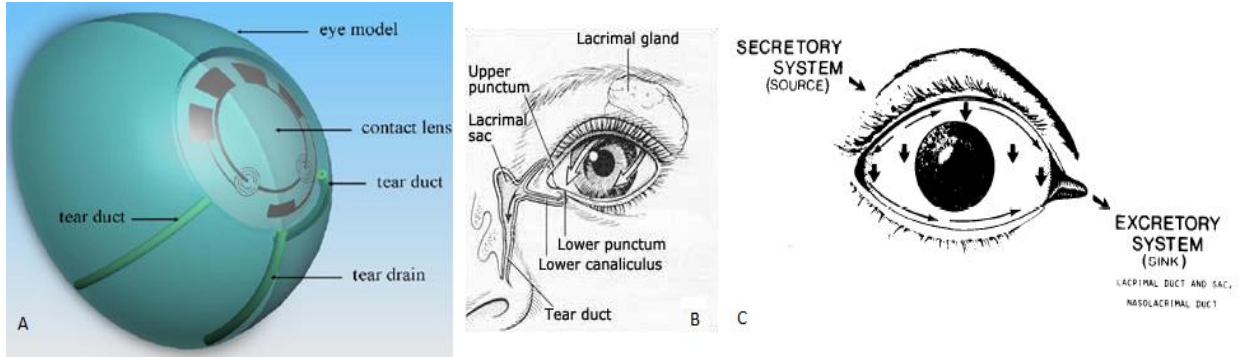


**Fig 2. Models of Tear Flow**

**A. Prototype-Associated Model [1] B. Diagonal Flow Model [8] C. Gravitational Tear Flow Model [7]**

Model 1, depicted in Figure 2A, was developed by Yao et al. [1], featured two diametrically placed side inlets and an outlet at the bottom of the contact lens. Model 2, in Figure 2B, features an inlet and outlet arc at opposite edges of the eye [8]. These capture the effect of tear displacement from the lacrimal glands to the lacrimal ducts. The associated tear flow is a mostly uniform front which moves diagonally over the eye. Model 3 (Figure 2C), described by Holly et al. [7], predicts a more uniform flow of fluid mediated by the tear distribution system of the eye. Newly released tears rapidly flow along the edges of the upper eyelid as a meniscus held by surface tension. Eye movements and blinking effect the distribution of the tears downward over the eye surface. This is implemented as semicircular arcs along the top and bottom of the model rim. The models presented are not incompatible, and a more complete model should account for all the factors that determine their respective tear flow dynamics.

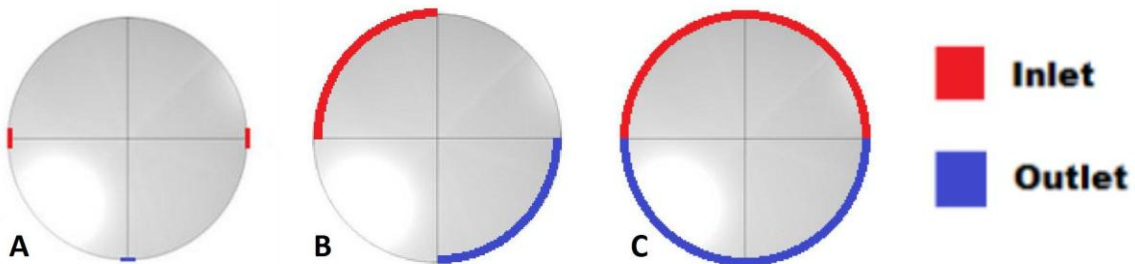


**Fig 3. Conditions for 3 Models of Tear Film Flow**

Locations of the inlets and outlets of the tear flow in the model are marked.

Figure 3 depicts the inlet-outlet configurations for Models 1, 2, and 3. The red marked regions represent the inlets where tears flow into the contact lens reservoir, while the blue marked regions represent the regions where tears flow out of the reservoir. These are the primary differences in the computational models because the physics modules implemented to represent the fluid and mass flows were the same.

## **Governing Equations, Boundary Condition, Initial Conditions and Properties**

### ***Governing Equations***

The Navier-Stokes equation describes the physics of the tear fluid flow in the problem. The body force term is dropped due to its insignificant effect on the solution and the transient term is dropped due to the establishment of steady state flow.

$$\rho(\mathbf{v} \cdot \nabla \mathbf{v}) = -\nabla p + \mu \nabla^2 \mathbf{v} \quad \text{Eq. 1}$$

Here  $\rho$  is density,  $\mathbf{v}$  is velocity,  $p$  is pressure, and  $\mu$  is viscosity.

The species equation describes the glucose mass transfer physics in the problem. The generation term is dropped due to the lack of glucose generation and degradation in the problem.

$$\frac{\partial c}{\partial t} + \mathbf{u} \cdot \nabla c = D \nabla^2 c \quad \text{Eq. 2}$$

Here  $c$  is the concentration of the mass modeled,  $t$  is the time variable,  $\mathbf{u}$  is the local fluid velocity, and  $D$  is diffusivity.

### ***Boundary Conditions***

#### Fluid flow:

The inlet fluid velocity is constant and set based the model. The outlet is set to zero pressure and it will allow both fluid and glucose to flow out of the geometry. All other surfaces of the geometry are set to have the no slip condition and zero fluid velocity.

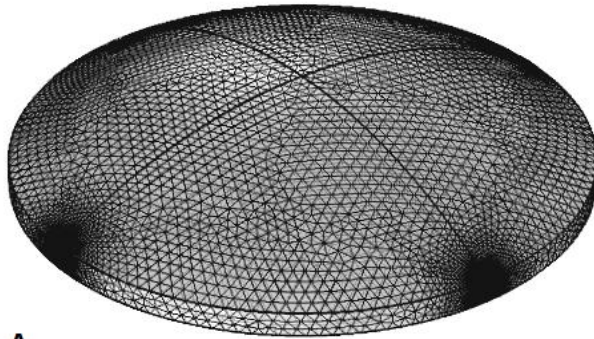
#### Mass transport:

The concentration of glucose at the inlets is equal to the concentration of glucose in produced tears. Glucose leaves the geometry with the outflow fluid and there is zero glucose flux at all other surfaces.

### ***Initial Conditions***

The entire domain has an initial condition of zero velocity and zero glucose concentration.

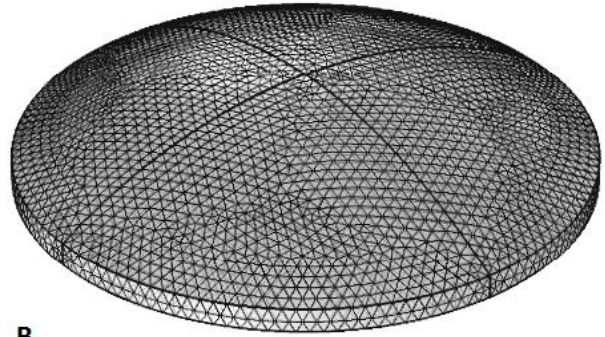
### Discretization



A

**Fig 4A. Model 1 Mesh**

Model 1 represented by a free-tetrahedral mesh composed of 145,741 elements. Note the higher element density at the inlets and outlet.



B

**Fig 4B. Model 2 and 3 Mesh**

Models 2 and 3 are represented by a free-tetrahedral mesh composed of 120,737 elements.

The mesh for Model 1 is different from the mesh of Models 2 and 3 due to the smaller dimensions of the inlets and outlets, which result in higher local velocities. A higher mesh element density was required to resolve these higher local velocities.

### Properties

Table 1 summarizes several parameters used to characterize aspects of tear flow and glucose transport. These parameters naturally vary between people, which prompted the inclusion of a parameter sensitivity analysis in the computational modeling results.

Property	Value
Glucose Diffusivity	$6.6 \cdot 10^{-8} \text{ m}^2/\text{s}$ [9]
Tear Density	1000 kg/m <sup>3</sup> [9]
Tear Viscosity	.001 Pa/s [10]

**Table 1. Property Values**

## RESULTS AND DISCUSSION

Several outcomes were achieved in the present study. First, three literature models were implemented as computational models of tear and glucose flow. Next, the results were validated by experimental data as well parameter sensitivity analysis. Finally, the contact lens design was optimized with respect to glucose sensor location.

### I. Computational Modeling of Tear Fluid Flow on the Eye Surface

Three computational models were generated to simulate the reservoir of fluid between a corneal surface of the eye and a contact lens. Each featured a different driving mechanism for the movement of liquid over the eye; Model 1 used two inlets and an outlet configured as in the paper by Yao et al., Model 2 used a physiologically consistent inlet and outlet corresponding to the lacrimal glands and lacrimal ducts respectively, and Model 3 used a downward gravity-driven flow in the upright lens. Model 1 was designed to recreate a physical model that had been built and characterized by another group [4]. Models 2 and 3 were alternative iterations designed to demonstrate the utility and flexibility of the simulation, each emphasizing a different driving force for tear movement on the eye.

To ensure the results could be compared to each other, Models 2 and 3 were configured to have approximately the same Peclet (Pe) dimensionless number as Model 1. This ensured their outputs would be on an appropriate scale. The Pe number, given by Eq. 3 below, was selected because it combines variables from fluid flow and mass transport to reduce the amount of redundant calculation needed to characterize the system.

$$Pe = \frac{uL}{D} \quad \text{Eq.}$$

Here,  $u$  is the local velocity,  $L$  is the characteristic length scale (defined as the inlet lengths from Figure 3), and  $D$  is the glucose diffusivity through tears. From the description of Model 1 provided by Yao et al., the characteristic Pe number was determined to be 12,500. The three models were used to generate fluid flow profiles and glucose concentration profiles.

Figure 5 demonstrates the fluid pressure distribution within the models at a selected time point. Each model had unique flow conditions, generating different pressure distributions.

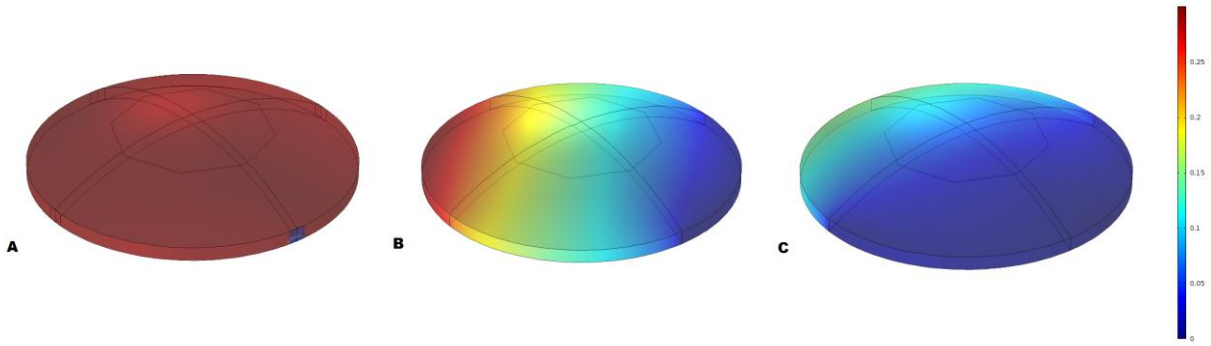


**Fig 5. Volume Plots of the Tear Fluid Pressure**

**A. Model 1**

There is a large pressure in the reservoir of the model that drives tear flow toward the outlet.

**B. Model 2**

The pressure decreases uniformly as the tear flow progresses diagonally across the contact lens.

**C. Model 3**

The pressure is highest at the center of top of the lens and decreases downward and along the edge of the lens.

Concentration profiles of glucose over time were then calculated for each model, demonstrated in animated Figures 6, 7 and 8. Note the differences in flow trajectory and speed between the models.

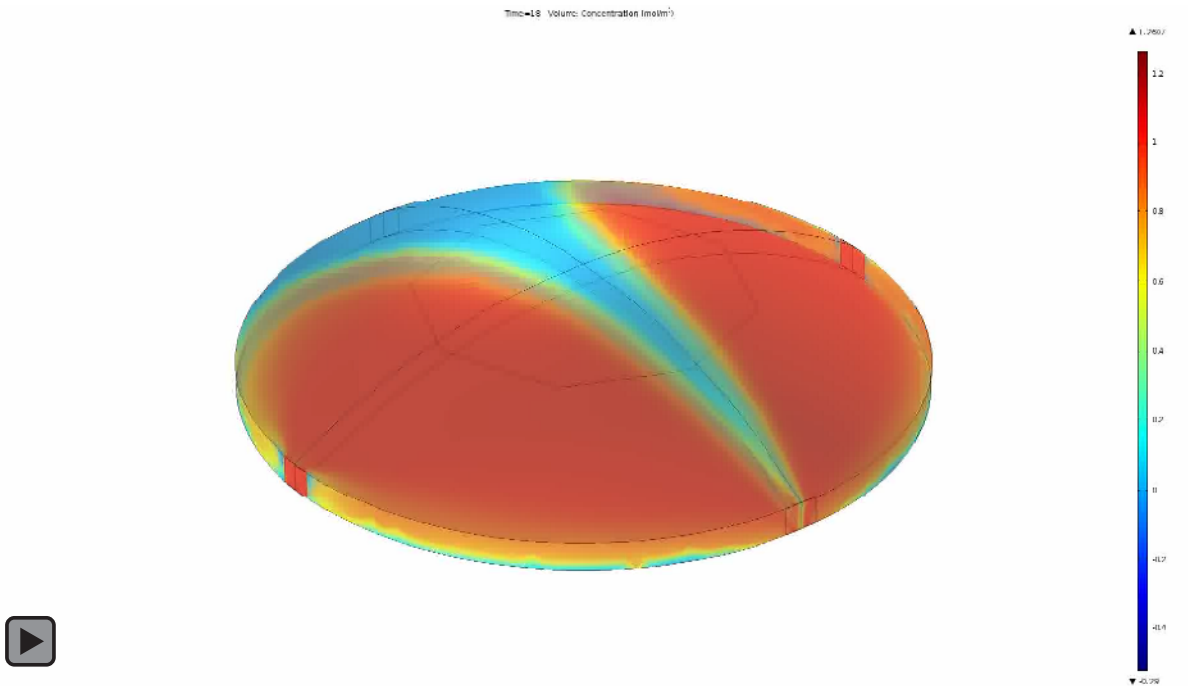


**Fig 6. Animation of Volume Plot of Glucose Concentration for Model 1**

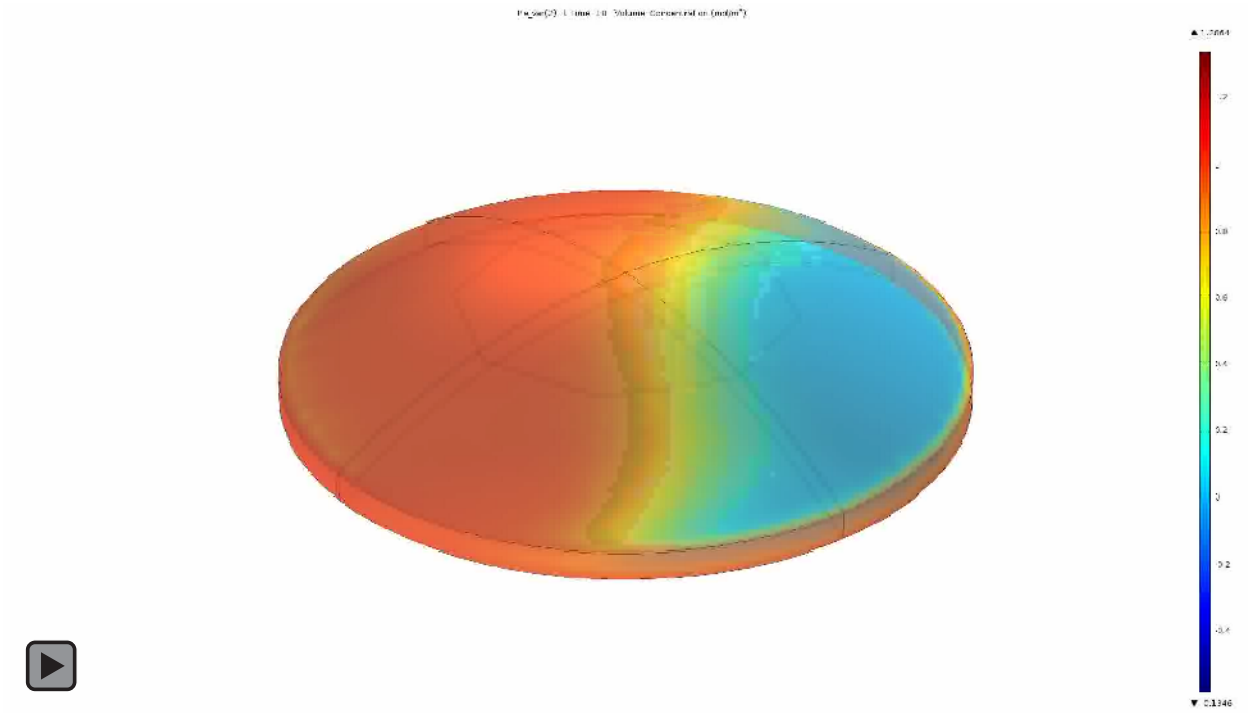


**Fig 7. Animation of Volume Plot of Glucose Concentration for Model 2**

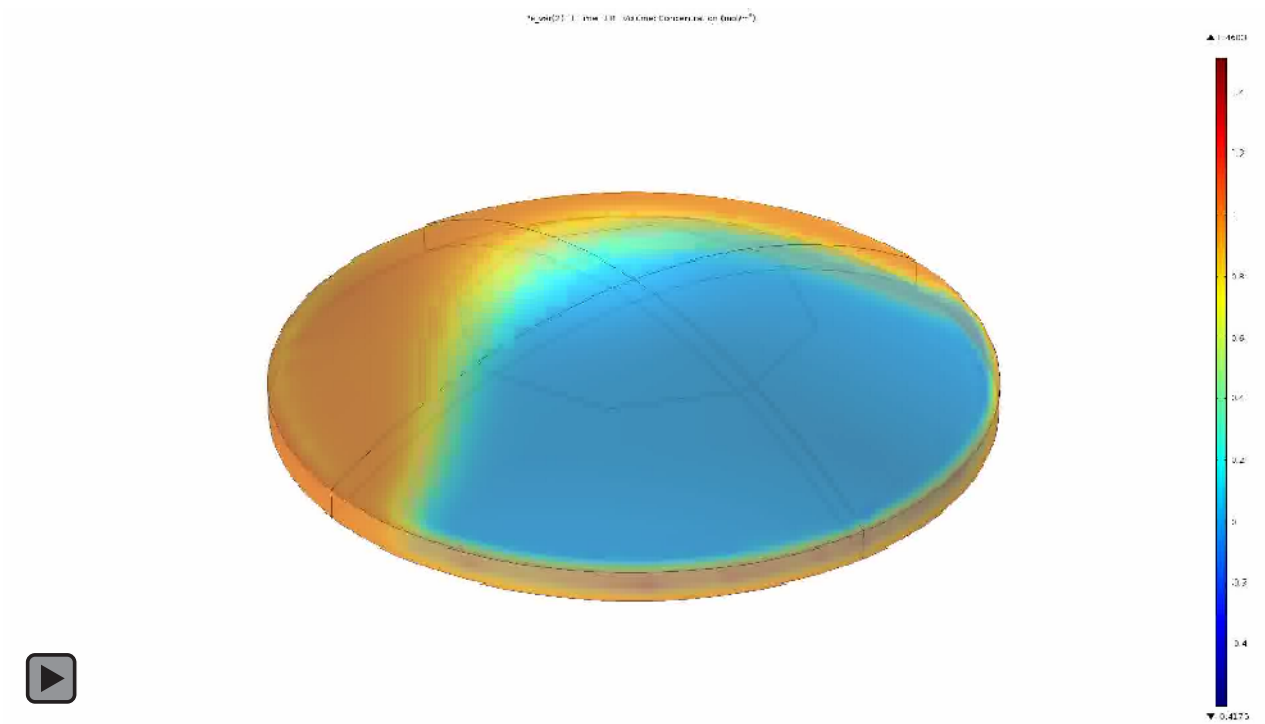


**Fig 8. Animation of Volume Plot of Glucose Concentration for Model 3**

These models of fluid and glucose movement were further analyzed to assess validity of the results.

## II. Validation of Computational Models

The stability of the models with respect to natural variations in Pe number of the models was established to ensure reliable, physically plausible results. The models were characterized through parameter sensitivity analysis which is summarized in Figure 9.

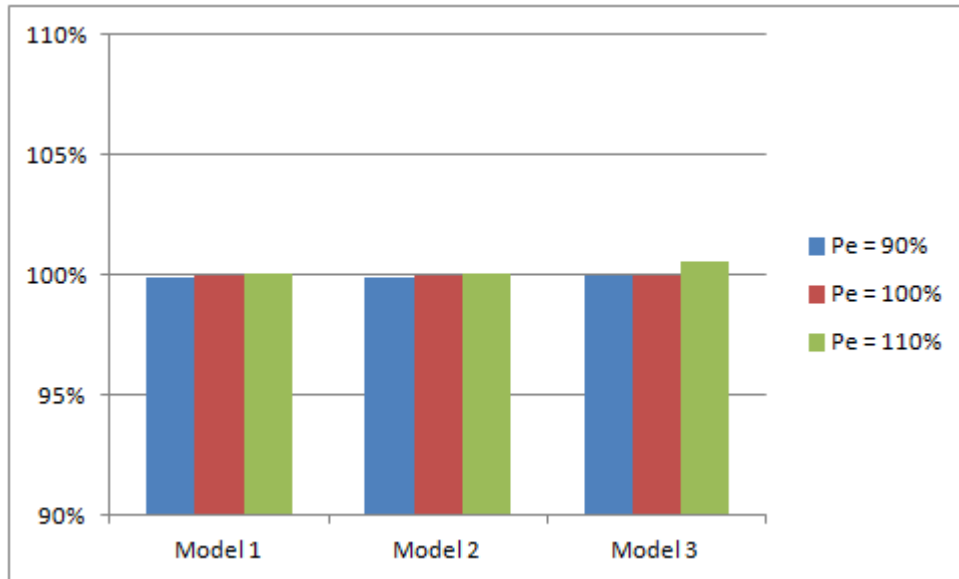


**Fig 9. Sensitivity of Glucose Concentration to Peclet Number**

All three models are relatively insensitive to moderate changes in the flow conditions and glucose diffusion jointly described by the dimensionless Peclet number.

The sensitivity of the two variables most important to the models, inlet flow rate and glucose diffusivity, were combined with the characteristic length scale (defined as the inlet arc length) into the Pe number. Parameters were adjusted to vary the Pe number by a range of 10% for each system. The models were determined to be relatively insensitive to Pe number variation. Glucose concentrations measured at the center of the contact lens at partial equilibration varied by less than 1% for Pe variation of  $\pm 10\%$ . All three models were determined to be stable with moderate variations in the diffusive flow conditions. Due to the insensitivity of each model to the Pe number, the variation between models can be directly attributed to the differences in inlet and outlet geometry in each model.

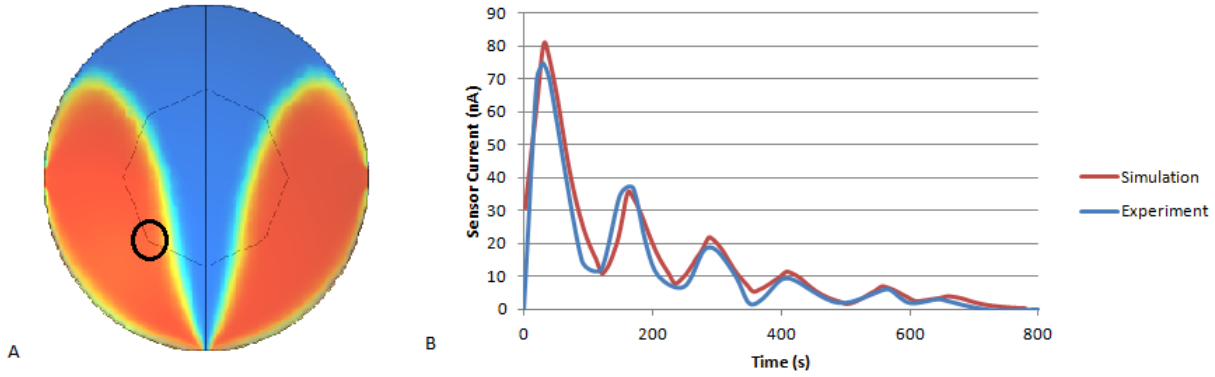


**Fig 10. Validation of Simulated Sensor Current in Model 1**  
**A. Schematic of Original Sensor Location B. Simulated and Experimental Sensor Current**

The concentration profile data from Model 1 could be validated against the data published on the original physical model reported by Yao et al. The point circled in Figure 10 shows the approximate location of the sensor in the original model, and the associated graph shows sensor current measured in both the computational simulation and experiment at this point [4]. The simulated sensor current was generated using the time variable input glucose concentration that could be linearly correlated to current as demonstrated by Yao et al. Additionally, the computed equilibration time of 20s is consistent with the experimental result, which also found a response time of 20s after taking into account the time delay of a fluid pump [4]. The response time was defined as the time needed for the point to reach 99% of its equilibrium glucose concentration. Note that in the physical model there is additional lag time between concentration equilibration and current detection, since there are intermediary steps such as the response time for the glucose sensor to report a signal that is not featured in the computational models. The model was concluded to be valid after assessing the reasonably matching current profile with variable glucose input and the similarity in equilibration time delay between the model and experiment.

### III. Optimization of Sensor Placement within the Contact Lens

A single combined model, shown in Figure 11, was generated from the results of the initial three models and then used to determine the ideal location of the sensor. This model weighed the conditions of each model equally to account for all the associated factors of tear flow.

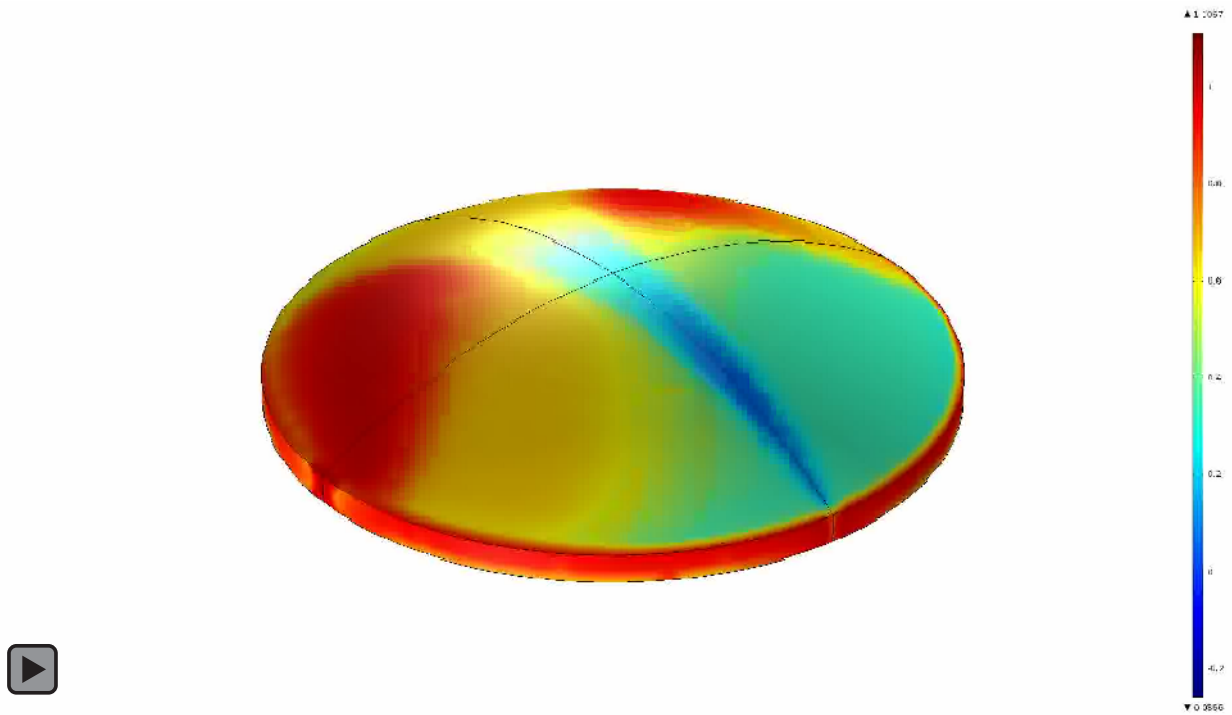


**Fig 11. Animation of Volume Plot of Glucose Concentration for Average of 3 Models**

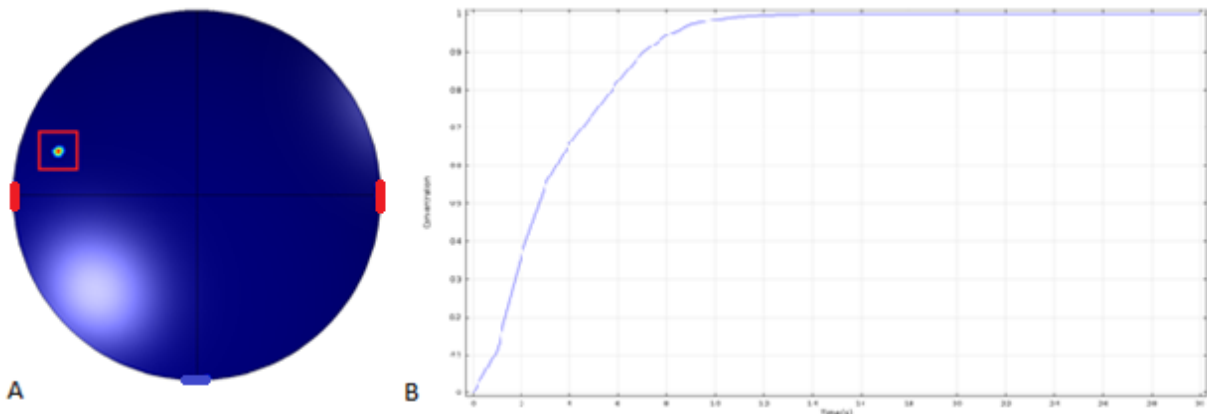


**Fig 12. Optimized Location of Glucose Sensor and Concentration Profile**  
**A. Optimized Location of Glucose Sensor B. Concentration Profile at Optimized Point**

The optimized location of the glucose sensor was determined by calculating the location at which the combined model equilibrated the quickest with respect to glucose concentration. As before, equilibration was defined as the time to reach 99% of the input concentration. The resulting location is a new point 5.3 mm left of and 1.7 mm above the center of the contact lens, which equilibrated after 14s in all three models. Note that this is for a right eye, but an equivalent lens for a left eye would be flipped horizontally. This point fits all three design criteria, avoiding the center of the contact lens to prevent occlusion of vision, providing enough physical space for the sensor and equilibrating in under 30s. As shown in Figure 11B, the equilibration time at this new point is 30% lower than the original value, with a response time of only 14 seconds.

## SUMMARY

Computational modeling is an effective tool for smart contact lens design. Three computational models were generated to model tear flow over the eye based on existing physical and theoretical models from literature. The computational models were validated by matching the results to experimental data collected from the physical model [4]. A single combined model was then generated to take into account the properties of all three original models. The results of the combined model suggest that a sensor placement in the upper, outer corner of the eye is ideal. This optimized model could be easily fabricated in the same manner as the original physical model, as only the location of the glucose sensor must be changed.

This optimized physical model can be made and then tested to verify the results of the optimized computational model. A more complete model could then be built using the full eye geometry as opposed to solely the contact lens. Additionally, future models using more sophisticated and physiologically accurate tear film models, such as thin film flow, could be made to provide more insight on equilibration times for tear fluids with respect to glucose concentration.

Future iterations of the smart contact lens prototypes could be improved using these computational models. However, before providing these devices to diabetic patients a number of obstacles must be overcome. In order to rigorously test the safety and effectiveness of smart contact lenses and gain FDA approval, clinical trials must be run with large samples of diabetic patients. Before this can be done, infrastructure must be made to mass produce these smart contact lens. Due to the similarity of production methods to microchips, scale up models are already available however they will need to be integrated with the contact lens manufacturing process. Following these two items, the cost of the smart contact lenses could be an issue for many patients and time will be needed for the manufacturing process to decrease costs to a reasonable level.

While wide use of smart contact lenses may be several years away for diabetic patients, the technology is a very promising solution. This alternative method for detecting glucose levels has many advantages over other methods, particularly its noninvasive nature. Most diabetic patients currently use finger pricking sensors or catheters integrated with glucose sensors which can be painful, inconvenient and carry a risk of infection. Smart contact lenses avoid all of these issues and are in a position to be the new standard once mass distribution of the lenses is possible.

## REFERENCES

1. Yao, H., Afanasiev, A., Lahdesmaki, I., & Parviz, B. A. (2011, January). A dual microscale glucose sensor on a contact lens, tested in conditions mimicking the eye. In *Microelectromechanical Systems (MEMS), 2011 IEEE 24th International Conference on* (pp. 25-28). IEEE.
2. Vashist, Sandeep Kumar. "Non-invasive glucose monitoring technology in diabetes management: A review." *Analytica chimica acta* 750 (2012): 16-27.
3. Tura, Andrea, Alberto Maran, and Giovanni Pacini. "Non-invasive glucose monitoring: assessment of technologies and devices according to qualitative criteria." *Diabetes research and clinical practice* 77. 1 (2007): 16-40.
4. Liao, Y., Yao, H., Lingley, A., Parvis, B., & Otis, B. (2012). A 3-uW CMOS Glucose Sensor for Wireless Contact-Lens Tear Glucose Monitoring. *IEEE Journal of Solid State Circuits*, 47(1), 335-344.
5. Ferrante do Amal, Carlos Eduardo, and Bernhard Wolf . "Current development in non-invasive glucose monitoring." *Medical Engineering & physics* 30.5 (2008): 541-549.
6. Tonyushkina, Ksenia, Nicole H. James. "Glucose Meters: A Review of Technical Challenges to Obtaining Accurate Results." *Journal of Diabetes Science and Technology* (2009) 971-981.
7. Holly, F., & Lemp, M. (1977). Tear physiology and dry eyes. *Survey of Ophthalmology*, 22(2), 69-87.
8. Dry Eye Syndrome. (n.d.). *North American Neuro-Ophthalmology Society*.
9. Epstein, Ami. "Solution Optimization and Physical Properties of Healthy Human Tears." *Contact Lens Spectrum* April (2010).
10. Ziegler, G. R., A. L. Benado, and S. S. H. Rizvi. "Determination of Mass Diffusivity of Simple Sugars in Water by the Rotating Disk Method." *Journal of Food Science* 52.2 (1987): 501-502.

## APPENDIX

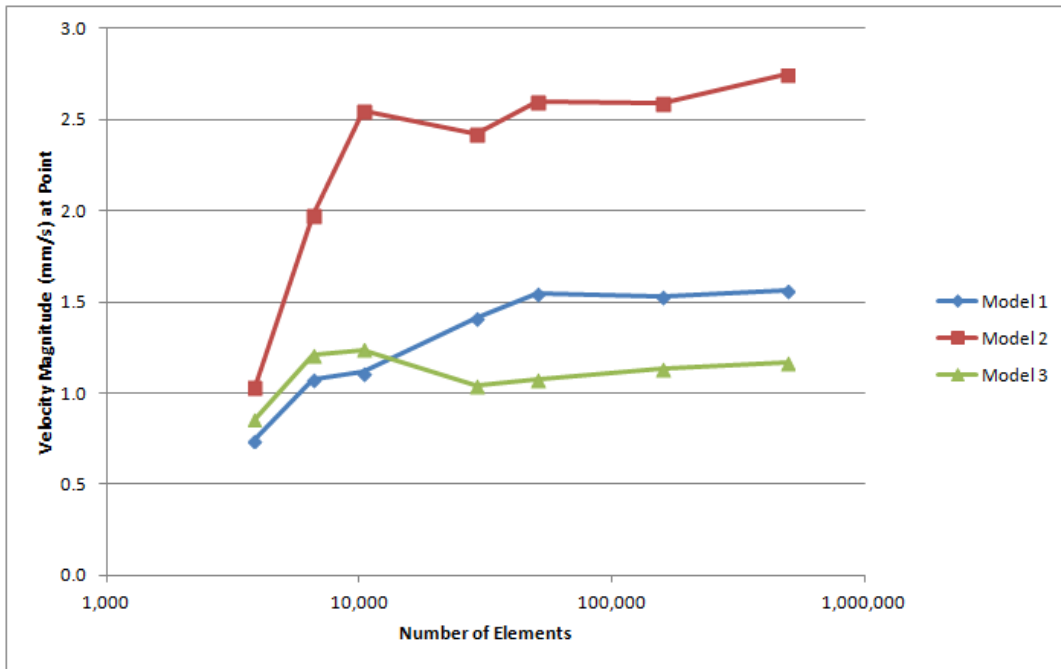


**Fig 13. Mesh Convergence Analysis**

The mesh converges after 50,642 elements for all three models. The plotted points are the velocity magnitude at the center of the lens in each model. At this resolution, the model becomes independent of mesh configuration.

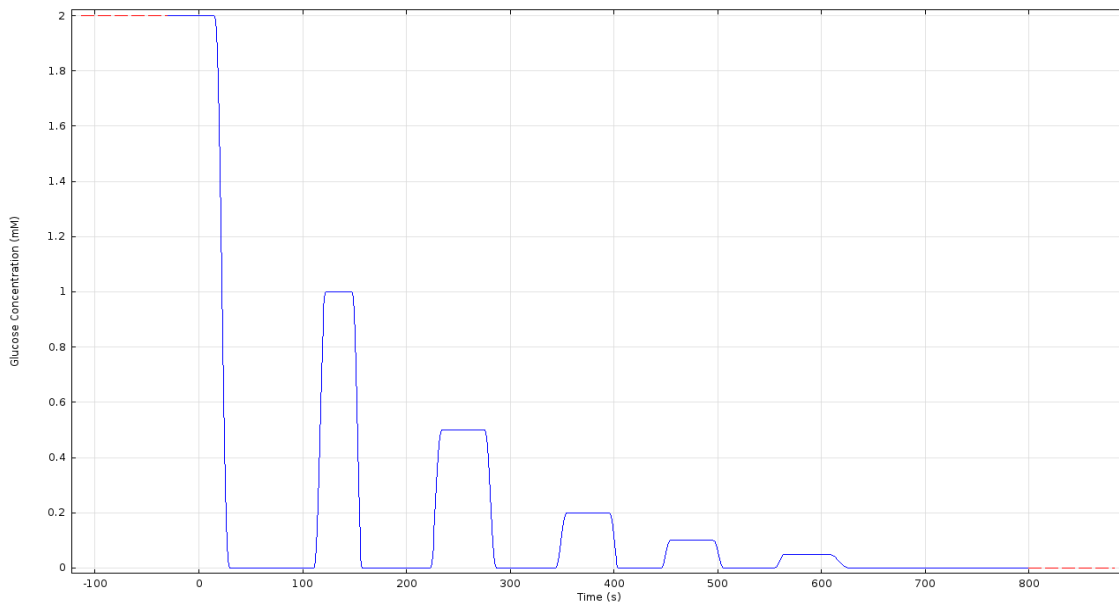


**Fig 14. Variable Glucose Input for Validation**

The glucose input function for the validation study replicates the input glucose concentrations used in the experiment with the original physical model [4]. The corresponding model outputs are plotted in red in Figure 10.